

See discussions, stats, and author profiles for this publication at: <https://www.researchgate.net/publication/278046473>

# Crystallization Kinetics of Indomethacin/Polyethylene Glycol Dispersions Containing High Drug Loadings

ARTICLE in MOLECULAR PHARMACEUTICS · JUNE 2015

Impact Factor: 4.38 · DOI: 10.1021/acs.molpharmaceut.5b00299 · Source: PubMed

---

CITATION

1

READS

39

## 3 AUTHORS, INCLUDING:



Tu Van Duong

University of Leuven

1 PUBLICATION 1 CITATION

[SEE PROFILE](#)



Jan Van Humbeeck

University of Leuven

368 PUBLICATIONS 6,819 CITATIONS

[SEE PROFILE](#)

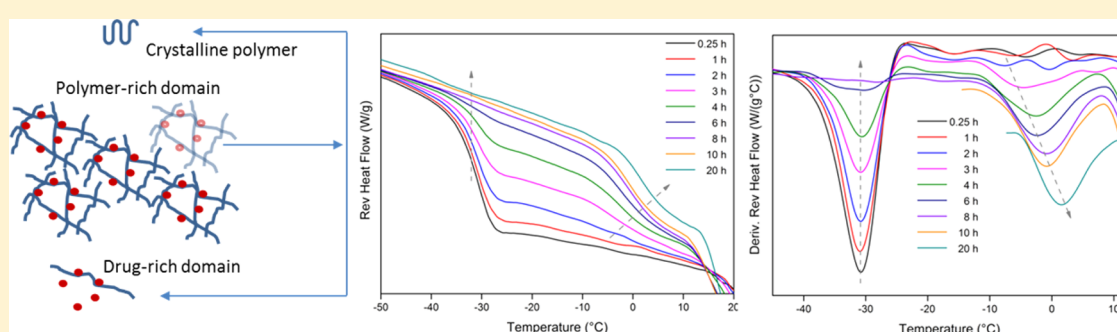
## Crystallization Kinetics of Indomethacin/Polyethylene Glycol Dispersions Containing High Drug Loadings

Tu Van Duong<sup>†,§</sup>, Jan Van Humbeeck<sup>‡</sup>, and Guy Van den Mooter<sup>\*,†</sup>

<sup>†</sup>Drug Delivery and Disposition, Department of Pharmaceutical and Pharmacological Sciences, KU Leuven, Campus Gasthuisberg O&N2, Herestraat 49 b921, 3000 Leuven, Belgium

<sup>‡</sup>Department of Materials Engineering, KU Leuven, Campus Arenberg, Kasteelpark Arenberg 44 b2450, 3001 Heverlee, Belgium

<sup>§</sup>Department of Pharmaceutics, Hanoi University of Pharmacy, 13-15 Le Thanh Tong, Hoan Kiem, Ha Noi, Vietnam



**ABSTRACT:** The reproducibility and consistency of physicochemical properties and pharmaceutical performance are major concerns during preparation of solid dispersions. The crystallization kinetics of drug/polyethylene glycol solid dispersions, an important factor that is governed by the properties of both drug and polymer has not been adequately explored, especially in systems containing high drug loadings. In this paper, by using standard and modulated differential scanning calorimetry and X-ray powder diffraction, we describe the influence of drug loading on crystallization behavior of dispersions made up of indomethacin and polyethylene glycol 6000. Higher drug loading increases the amorphicity of the polymer and inhibits the crystallization of PEG. At 52% drug loading, polyethylene glycol was completely transformed to the amorphous state. To the best of our knowledge, this is the first detailed investigation of the solubilization effect of a low molecular weight drug on a semicrystalline polymer in their dispersions. In mixtures containing up to 55% indomethacin, the dispersions exhibited distinct glass transition events resulting from amorphous–amorphous phase separation which generates polymer-rich and drug-rich domains upon the solidification of supercooled polyethylene glycol, whereas samples containing at least 60% drug showed a single amorphous phase during the period in which crystallization normally occurs. The current study demonstrates a wide range in physicochemical properties of drug/polyethylene glycol solid dispersions as a result of the complex nature in crystallization of this system, which should be taken into account during preparation and storage.

**KEYWORDS:** solid dispersions, crystallization, kinetics, crystalline, amorphous, indomethacin, polyethylene glycol, drug loading, phase separation, modulated differential scanning calorimetry, X-ray diffraction

### INTRODUCTION

Solid dispersion is a potential formulation strategy to improve the solubility and dissolution rate of poorly water-soluble compounds. Despite promising benefits, a primary concern that hampers the wide application is the reproducibility and consistency of physicochemical properties of the systems during production and storage which results in variations in the bioavailability. Solid dispersions are composed of an active pharmaceutical ingredient (API) dispersed in a pharmacologically inert matrix made up of highly water-soluble amorphous or semicrystalline polymers.

Polyethylene glycol (PEG) is the most commonly used semicrystalline polymer for preparation of solid dispersions since it exhibits several advantageous features such as high water-solubility, low melting point, good solubility in many

organic solvents as well as its ability to solubilize drugs and improve wettability, which eventually can lead to enhanced dissolution and bioavailability.<sup>1</sup> Solid state properties of PEG as well as PEG-based solid dispersions have been extensively investigated to understand the microstructure and fundamental physicochemical characteristics that may influence the dissolution behavior of the systems. It has been found that the microstructure of solid dispersions made up of APIs and PEG is inherently complex and there is a huge variation in crystallization behavior, location and domain size of APIs. For

Received: April 19, 2015

Revised: June 5, 2015

Accepted: June 9, 2015

Published: June 9, 2015

instance, nifedipine<sup>2</sup> and haloperidol<sup>3</sup> were crystalline whereas oxazepam<sup>4</sup> and loratadine<sup>5</sup> were dissolved in the PEG matrix.

Depending on the crystallization tendency of the API and the interaction between the API and PEG, the API can be located in interlamellar, interfibrillar, or interspherulitic regions or some combination of these regions in the PEG matrix, yielding different microstructures, which in turn gives rise to various material properties. Zhu et. al observed that haloperidol was located in the interfibrillar regions of PEG, whereas aceclofenac and chlorpropamide appeared to exist within at least two regions of the polymer, namely, interlamellar and interfibrillar region, with domain sizes of nanometric and micrometric scale, respectively.<sup>3</sup> This research group also reported that the difference in the crystallization temperature and composition of solid dispersions made up of naproxen and PEG resulted in distinct overall crystallization rates of naproxen, which in turn varied the size and spatial distribution of API in the polymer matrix. This difference in microstructure had a substantial impact on dissolution behavior of the system.<sup>5</sup>

Furthermore, the microstructure of these systems is likely to change as a function of time due to the crystallization of API or polymer.<sup>3</sup> The properties of additives have been found to affect the crystallization of PEG. Unga et al. showed that crystallization behavior and hence solid state structure of PEG considerably depends on the physicochemical properties of the lipid presented: higher degree of intercalation of lipid into PEG lamellae induced larger lamellar thickness and increased the folded PEG fraction.<sup>6</sup> The inherent complexity in microstructure of API/PEG solid dispersions requires further elucidation to better understand this type of solid dispersions.

Studies on solid dispersions in general and API/PEG systems in particular have mainly focused on how carriers affect properties of APIs. However, the influence of APIs on the properties of carriers is also of practical and fundamental importance because it has been reported that introduction of other polymers such as copolymer of ethylene/methacrylic acid and styrene-*co*-hydroxystyrene copolymer, which form strong intermolecular interactions with PEG could significantly reduce crystal growth rates of PEG in polymer blends.<sup>7</sup> The crystallization behavior of PEG in the presence of high molecular weight additives, that is, other polymers such as poly(methyl methacrylate) or polyvinyl acetate has been widely characterized.<sup>7–10</sup> However, only few studies have been conducted to investigate how the crystallization of PEG is affected in mixtures containing PEG and low molecular weight additives.

Recent studies have shown that depending on the specific API, the presence of PEG either accelerated, decreased or had no influence on the crystallization process of APIs. On the other hand, the APIs were also found to influence the crystallization rate of PEG.<sup>3,11</sup> The crystallization of PEG in the presence of benzocaine and ibuprofen was much slower than that of pure PEG, whereas for systems containing haloperidol and fenofibrate, PEG crystallized as fast as the neat material. The microstructure of these systems might be influenced as a result of the change in crystallization rate of PEG. Therefore, it is important to further investigate the crystallization behavior of not only the API but also the carrier because they can both affect the microstructure and physicochemical properties of solid dispersions and subsequently influence the dissolution behavior and bioavailability.

As solid dispersions of poorly water-soluble compounds are mostly targeted for the oral route of administration,

encapsulating them in the form of capsules or compressing into tablets are the foremost preferences. Usually, a tablet or capsule of a total weight about 1 g is considered as the upper limit for the mass that allows for ease of swallowing by a normal adult patient without discomfort. Suppose that the drug loading of a solid dispersion is 5%, doses higher than 50 mg would not be feasible with this formulation strategy.<sup>1</sup> In addition, to formulate a solid dispersion, a large amount of excipients might be required. For instance, 270 mg of microcrystalline cellulose is needed to formulate 30 mg of mefenamic acid/PEG 3350 solid dispersion into a tablet with desired dissolution performance.<sup>12</sup> Likewise, to process 100 mg of solid dispersion of indomethacin/PEG 6000 in the formulation of tablets, Ford et al. had to add 506 mg of excipients including calcium hydrogen phosphate, sodium starch glycolate, and magnesium stearate.<sup>13</sup> The use of such a high ratio of excipients dramatically increases the mass and hence the size of tablet or capsule and might, therefore, be impractical. With respect to pill burden, formulation scientists will attempt to achieve as high a drug loading as possible to overcome the practical limit of the dosage form size.

In solid dispersions, most API–carrier systems are only partially miscible, with phase separation occurring as the drug weight fraction increases. Hence, solid dispersions of API and PEG have been mainly studied with low drug loading and in most of the cases not more than 50%.<sup>14</sup> Thus far, there have been no studies of semicrystalline polymer-based solid dispersions containing higher drug loadings.

Considering the importance of the crystallization process in determining the properties of the resultant solid dispersions, and the necessity to get a deeper insight into the crystallization process of semicrystalline polymers during the formation of solid dispersions to improve the reproducibility and consistency of product qualities, the purpose of this work was to investigate the crystallization kinetics of solid dispersions made up of the model API indomethacin and PEG 6000 containing high drug loadings.

## EXPERIMENTAL SECTION

**Materials.** The model API,  $\gamma$  indomethacin (IMC), and PEG 6000 were purchased from Fagron (Saint-Denis, France) and Sigma-Aldrich (Geel, Belgium), respectively. All chemicals were used without further purification.

**Sample Preparation.** Dispersions made up of IMC and PEG were prepared by heating the mixture of the two components to 165 °C (above the melting temperatures of both components) to ensure complete melting, followed by solidification. All samples were analyzed without further sample processing. Samples were sealed in the cell of a Q2000 modulated differential scanning calorimeter (DSC) (TA Instruments, Leatherhead, U.K.) or stored over phosphorus pentoxide between measurements in a sealed desiccator to prevent the influence of atmospheric moisture.

The molten mixtures of drug and polymer at 165 °C were cooled at various rates of 1, 2, and 20 °C/min to investigate the influence of cooling rate on the crystallization of the dispersions.

Samples for crystallization kinetics analysis were prepared in aluminum DSC pans (TA Instruments) by keeping the mixtures of IMC and PEG at 165 °C during 3 min before cooling to 5 °C at the cooling rate of 2 °C/min. Following preparation, samples were stored in a sealed desiccator over phosphorus pentoxide at 5 °C and analyzed at predetermined

time intervals to monitor the crystallization kinetics of the dispersions.

#### Modulated Differential Scanning Calorimetry (MDSC).

Thermal properties of dispersions were analyzed using a Q2000 MDSC (TA Instruments) purged with inert dry nitrogen gas at a flow rate of 50 mL/min and connected to a refrigerated cooling system RCS90 (TA Instruments). Temperature scale was calibrated and validated using indium and *n*-octadecane standards. Melting enthalpy was calibrated and validated using indium. Sapphire disks were used to calibrate the heat capacity. Validation was performed by comparing the measured heat capacity with the theoretical values at 46.85 °C.

The samples were crimped in aluminum DSC pans and subjected to heating from -75 to 165 °C using an underlying heating rate of 5 °C/min with a modulating amplitude of 0.636 °C and a period of 40 s. All samples were analyzed in duplicate. The data were acquired using Thermal Advantage software and analyzed by Universal Analysis software (version 4.4, TA Instruments). The value of  $T_g$  presented was the midpoint of the transition in the reversing heat flow signal.

**X-ray Diffraction (XRD).** Diffractograms of samples were recorded by using an automated X'pert PRO diffractometer (PANalytical, Almelo, The Netherlands) equipped with a copper K $\alpha$  radiation ( $\lambda = 0.15418$  nm) source. The voltage and current were set at 45 kV and 40 mA, respectively.

Samples were mounted on a sample holder and scanned over a range of  $4^\circ \leq 2\theta \leq 40^\circ$  using a step size of  $0.0167^\circ$  and counting time of 200 s. The X'pert Data Collector (PANalytical, Almelo, The Netherlands) was used for data acquisition, and data analysis was performed by using the X'Pert Data Viewer and X'Pert HighScore Plus (PANalytical, Almelo, The Netherlands).

In order to investigate the influence of temperature on crystallization of solid dispersions, mixtures of IMC and PEG were mounted on a TTK 450 thermostated sample holder unit (Anton Paar, Graz, Austria), kept isothermal at 165 °C during 3 min, followed by cooling to 5, 10, 15, and 20 °C at a cooling rate of 2 °C/min; then diffractograms at these temperatures were recorded.

**Macroscopic Crystallization Kinetics.** The crystallinity of PEG was used as an indicator to monitor the crystallization process of the polymer. The crystallinity of PEG in the sample at time  $t$ , denoted as  $\phi_t$ , is given by the following equation

$$\phi_t = 100 \times \frac{\Delta H}{\Delta H_0 \times \chi_p} \quad (1)$$

where  $\Delta H$  and  $\chi_p$  are the heat of fusion at time  $t$  and weight fraction of PEG in the sample, respectively;  $\Delta H_0$  is the heat of fusion of perfect PEG crystals, whereby a value of 205 J/g is used.<sup>15</sup>

The crystallinity data are fitted to the Avrami equation<sup>16–18</sup> by nonlinear curve fitting using Origin 8.5 (OriginLab Corp., Northampton, U.S.A.)

$$\phi_t = 1 - e^{-Kt^n} \quad (2)$$

where  $K$  is the overall crystallization rate constant (i.e., it contains contributions from both nucleation and crystal growth steps), which relates to the crystallization conditions, and  $n$  is the Avrami exponent which indicates the geometry of crystal growth.

## RESULTS

**Solubilization of PEG in Amorphous IMC.** In order to investigate the solubilization effect of supercooled amorphous IMC on PEG, mixtures of drug and polymer containing various IMC loadings were kept isothermal at 165 °C during 3 min before cooling to -75 °C at the cooling rate of 20 °C/min and subsequent reheating to 165 °C at 5 °C/min. These parameters were kept unchanged for all experiments.

Figure 1 shows that when the weight fraction of IMC increased, the crystallization and melting peaks of PEG became

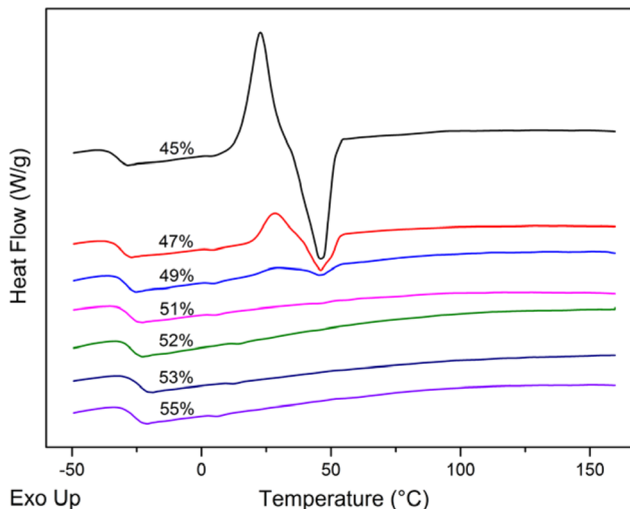


**Figure 1.** DSC thermogram with heat flow signal vs. temperature for samples containing different drug loadings upon heating after being cooled from the melt.

smaller and eventually disappeared in samples containing at least 52% IMC. No crystallization signal of PEG was observed in all samples upon cooling (data not shown). When the weight fraction of IMC increased to higher than 52%, the system was more stable, and consequently, no PEG crystallized upon heating, which led to the disappearance of the melting peak of PEG. These data indicated the transformation of crystalline PEG into the amorphous state in supercooled amorphous IMC.

It is well known that PEG is a highly crystallizable polymer and pure PEG crystallizes extremely fast with an induction time of only few seconds and the complete crystallization of PEG is achieved within less than 2 min.<sup>11</sup> The presence of APIs such as ibuprofen or fenofibrate was found to be able to delay the crystallization process of PEG, yet PEG was still observed to crystallize rapidly.<sup>7,11</sup> The current study is indeed the first detailed investigation of the solubilization effect of a low molecular weight drug on a semicrystalline polymer in their dispersions, and this phenomena was also recently observed by Vasa et al.<sup>19</sup> This effect still took place when samples were prepared at much lower cooling rate of 1 °C/min as long as amorphous IMC was generated upon cooling.

**Composition-Dependent Crystallization Temperature.** In samples containing less than 52% IMC, PEG crystallized upon reheating (Figure 2). The crystallization onset temperature of PEG increased with %IMC: it was -17, 7, and 15 °C in 40%, 45%, and 50% IMC samples, respectively. When drug loading increased to 52%, no crystallization peak of PEG was detected. These data confirmed that amorphous PEG was more stable at higher drug loading.

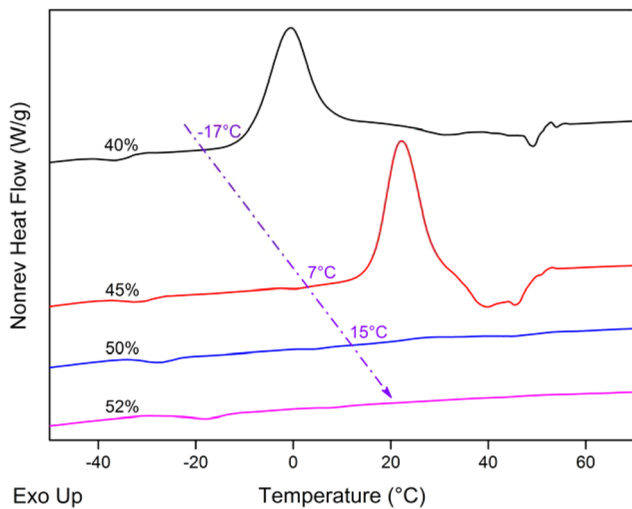


**Figure 2.** Crystallization temperature of PEG in dispersions containing various drug loadings.

**Composition-Dependent Glass Transition Temperature ( $T_g$ ) Shifting.** A clear trend was observed that  $T_g$  of dispersions increased with %IMC because  $T_g$  of IMC is much higher than that of PEG (Figure 3). Figure 4 shows the change

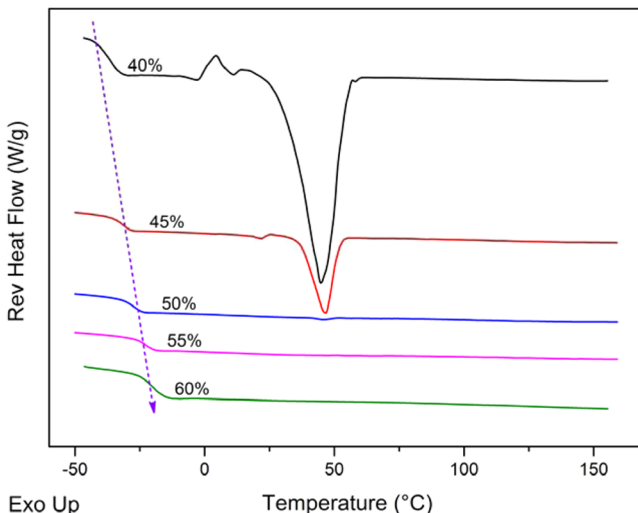


**Figure 3.** DSC thermogram with reversing heat flow signal vs. temperature for samples containing different drug loadings upon heating after being cooled from the melt.

of  $T_g$  of the system as a function of drug loading. There was a strong linear correlation ( $R^2 = 0.99$ ) between  $T_g$  of the system and %IMC. The single and sharp  $T_g$  points to the miscibility of the system.

PEG has been reported to exhibit a  $T_g$ , which depends on the molecular weight. By using broadband proton nuclear magnetic resonance, Faucher et al. showed that  $T_g$  of PEG increased from  $-49\text{ }^\circ\text{C}$  for PEG 400 to a maximum of  $-20\text{ }^\circ\text{C}$  for PEG 6000 and then decreased with molecular weight.<sup>20</sup> However, in the current study, dispersions containing IMC and PEG 6000 displayed  $T_g$ 's well below  $-20\text{ }^\circ\text{C}$  (Figure 4), suggesting that the  $T_g$  of pure PEG 6000 must be much lower than  $-20\text{ }^\circ\text{C}$ .

**Cooling Rate-Dependent Crystallization of PEG.** The influence of different cooling rates of 1, 2, and  $20\text{ }^\circ\text{C}/\text{min}$  on crystallization of PEG is shown in Figure 5. It was apparent that

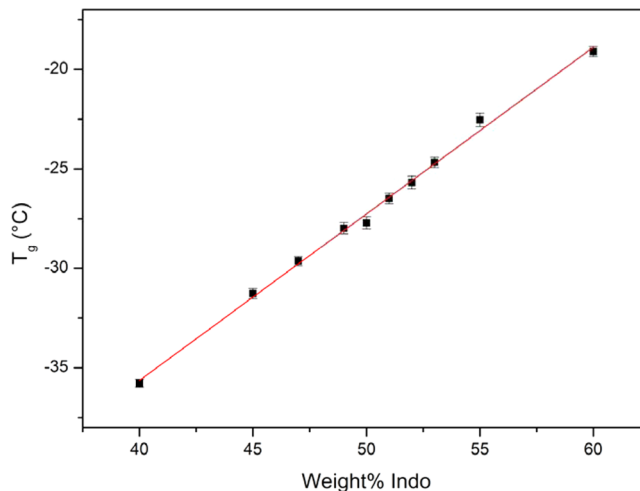


**Figure 4.** Change in  $T_g$  of solid dispersions with weight fraction of IMC.

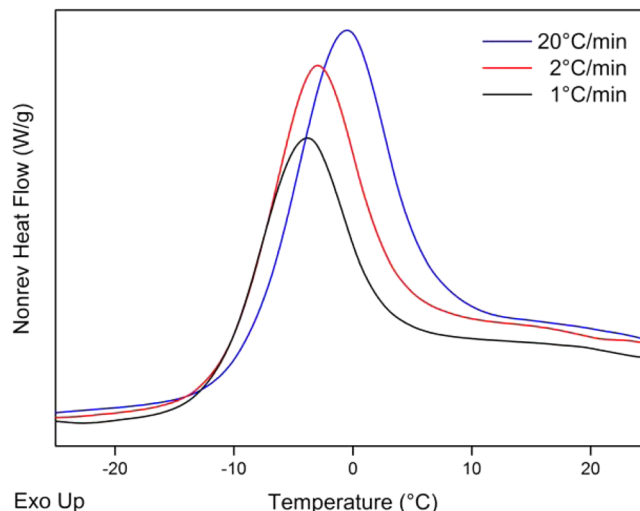


**Figure 5.** Crystallization of PEG in the sample containing 40% IMC upon heating after being cooled at 1, 2, and  $20\text{ }^\circ\text{C}/\text{min}$ .

after being cooled at lower rates, less PEG crystallized upon heating. At lower cooling rates, more PEG already crystallized during the cooling step because PEG had longer time for crystallization. Consequently, the amount of PEG crystallized upon heating became smaller. These data are consistent with previously reported observations that for PEG, increasing cooling rates resulted in inhibition of nucleation of the melt and reduction in crystal growth rates.<sup>21,22</sup> The same effect of cooling rate was also detected for IMC: the physical stability of amorphous IMC was found to increase as a function of cooling rate because at lower cooling rate, more nuclei were present in the resulting amorphous IMC as this amorphous domain had existed in the supercooled state for a longer time.<sup>21,23</sup>

**$T_g$  Change upon Reheating.** Similar to the crystallization of PEG, the  $T_g$  of dispersions also depended on the cooling rate. After being cooled at lower rates, dispersions of PEG and IMC exhibited slightly higher  $T_g$  and lower change in heat capacity at  $T_g$  ( $\Delta C_p$ ) upon reheating (Figure 6 and Table 1). At lower cooling rates, more PEG already crystallized during cooling whereas IMC had not yet crystallized. Therefore, the relative ratio of amorphous IMC/amorphous PEG increased and  $T_g$  of dispersions shifted to higher values. In addition, due

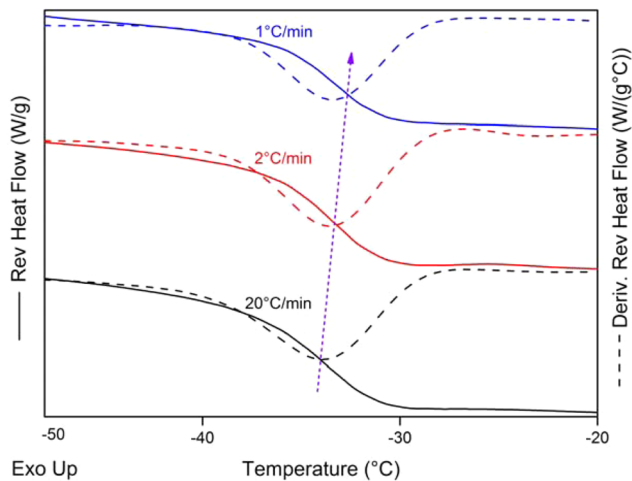


**Figure 6.** DSC thermogram with reversing and derivative reversing heat flow signal vs. temperature of the sample containing 40% IMC upon heating after being cooled at 1, 2, and 20 °C/min (reversing heat flow—solid lines, derivative reversing heat flow—dashed lines).

**Table 1. Experimental  $T_g$  Midpoint,  $T_g$  Width,  $\Delta C_p$  and AUC for the Sample Containing 40% IMC upon Heating after Being Cooled at Different Rates**

cooling rate (°C/min)	$T_g$ midpoint (°C)	$\Delta C_p$ (J/g°C)	$\Delta T_g$ width (°C)	AUC <sup>a</sup> (mJ/(g°C))
1	-34.77	0.63	17.88	507.18
2	-35.66	0.74	19.96	617.40
20	-35.77	0.79	22.63	670.20

<sup>a</sup>AUC: the area of the peak across glass transition temperature in the derivative reversing heat flow signal as a function of temperature, is a measure of the amorphous content in solid dispersions.

to the crystallization of PEG, the total degree of amorphylicity of the dispersions decreased which led to a smaller  $\Delta C_p$  and area under the derivative reversing heat flow peak (AUC) at  $T_g$ .

The span of the glass transition region ( $T_g$  width) was slightly increased at higher cooling rates, suggesting the induction of inhomogeneity in the dispersions when samples were rapidly cooled.<sup>24</sup>

**Crystallization Kinetics of PEG in Dispersions.** Samples for crystallization kinetics analysis were prepared by keeping the mixtures of IMC and PEG at 165 °C during 3 min in aluminum DSC pans before cooling to 5 °C at the cooling rate of 2 °C/min. Because amorphous dispersions became noticeably stable upon fast cooling, a relatively low cooling rate of 2 °C/min was selected, otherwise the crystallization period would be too long for monitoring. Following preparation, samples were stored at 5 °C and analyzed at predetermined time intervals to monitor the crystallization kinetics of the dispersions.

A visualization of crystallization of samples containing different compositions of PEG/IMC is illustrated in Figure 7. It can be seen that changing the weight fraction of IMC in samples resulted in a huge difference in crystallization behavior of PEG. Figure 8 depicts the crystallization kinetics of PEG in samples containing various IMC loadings. The crystallization rate of PEG is inversely proportional to the weight fraction of IMC, that is, PEG crystallized more slowly as the weight fraction of IMC increased. Crystallization parameters including induction time (the time elapsing before the melting peak of PEG appeared, denoted as  $t_{ind}$ ), end point of crystallization (the time when crystallization of PEG appeared to be complete

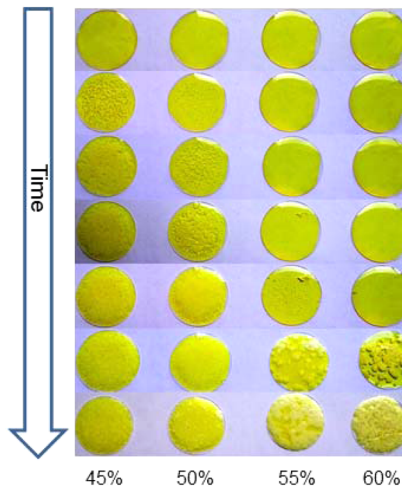


**Figure 7.** Visualization of the crystallization of samples containing different drug loadings.

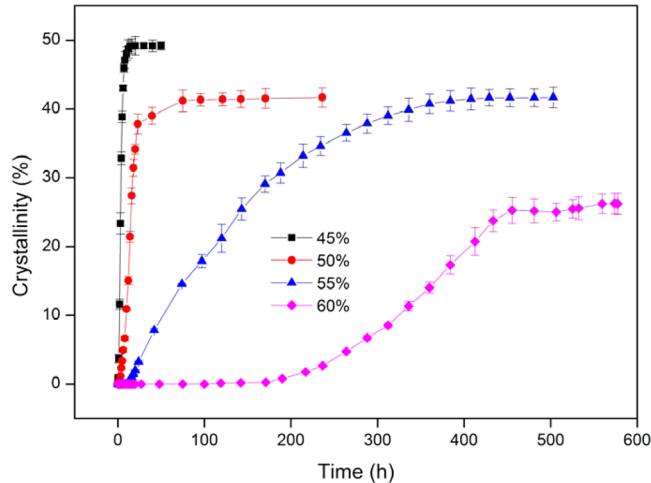


**Figure 8.** Crystallization kinetics of PEG in samples containing different drug loadings.

which was evident by the plateau of melting peak area, denoted as  $t_{end}$ ), and the time taken for half of the crystallization to develop ( $t_{1/2}$ ) of samples containing different IMC loadings are summarized in Table 2.

It is evident that in samples containing 45% and 50% IMC, the PEG crystallized immediately without induction time. When the weight fraction of IMC increased to 55% and 60%, the induction time dramatically increased to 12 and 120 h, respectively. In addition to the induction time,  $t_{1/2}$  and  $t_{end}$  also suggested that the period of crystallization was much longer in

**Table 2. Crystallization Parameters for Samples Containing Different Drug Loadings**

drug loading <sup>a</sup>	45%	50%	55%	60%
$t_{ind}$ (hour)	0	0	12	120
$t_{1/2}$ (hour)	3	14	108	240
$t_{end}$ (hour)	16	121	400	440
$\phi_{end}$ (%)	49.2	41.5	41.6	26.2
Avrami exponent	1.95	2.45	1.38	5.16

<sup>a</sup> $t_{1/2}$  and  $t_{end}$  do not include the induction time;  $\phi_{end}$  is crystallinity of PEG at  $t_{end}$

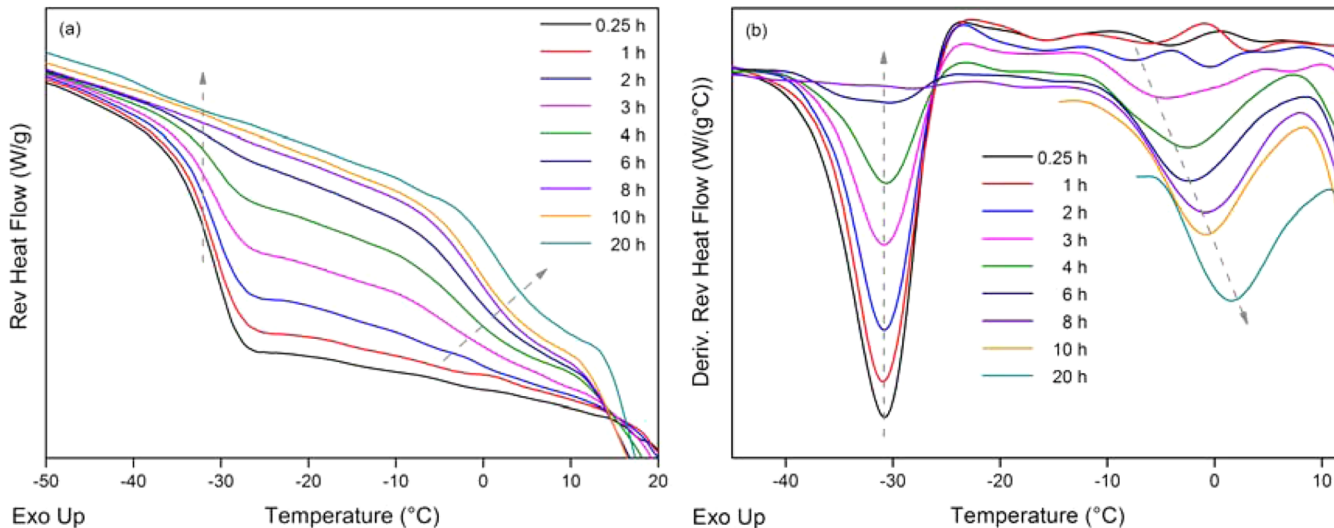


**Figure 9.** DSC thermogram with (a) reversing heat flow signal and (b) derivative reversing heat flow signal vs. temperature of the sample containing 45% IMC stored for different time periods at 5 °C.

samples containing a higher amount of IMC. In 45% IMC sample, it took only 3 h for 50% amorphous PEG to transform into the crystalline state and  $t_{1/2}$  drastically increased approximately 5, 36, and 80 times in samples containing 50%, 55%, and 60% IMC, respectively. An increase of drug loading by 5% from 55% resulted in 10 times longer induction time (12 h vs 120 h). However, when PEG started to crystallize, the rate of crystallization in samples containing 55% and 60% was more or less comparable and the crystallization process was in both cases completed after approximately 400 h.

At the end point, the crystallinity of PEG in samples containing 45%, 50%, 55%, and 60% IMC was ca. 50%, 40%, and 25% of that of perfect PEG crystals, respectively. This implied that the other fraction of PEG still existed in the amorphous state in dispersions with amorphous IMC, which was represented by the yellow color of samples at  $t_{end}$  (Figure 7) or by a  $T_g$  in DSC thermograms; this amorphous fraction increased with %IMC.

Fitting crystallinity data to the Avrami model (eq 2) gives different Avrami exponent values, suggesting various growth geometries of PEG crystals.<sup>25</sup> At 45% and 55% drug loading,  $1 \leq n \leq 2$ , indicating one-dimensional, linear growth of crystals similarly to the crystal growth for pure PEG,<sup>11</sup> whereas for samples containing 50% IMC,  $2 \leq n \leq 3$  suggesting two-dimensional, plate-like growth. When drug loading increased to 60%, sheaf-like growth of PEG crystals was exhibited which related to the observation reported for crystallization of PEG at low temperature.<sup>25,26</sup> Figure 7 shows that at the end point, samples exhibited notably different appearances. Dispersions containing higher weight fraction of drug displayed the formation of larger sheaf-like structure. This might be an indication of distinct microstructures evolved in dispersions containing various drug loadings, which resulted from the changing crystallization rate of PEG.

**Time-Dependent  $T_g$  Shifting.** An interesting shift in  $T_g$  of the dispersions as a function of time was observed while investigating the crystallization kinetics of PEG. The sample containing 45% IMC was kept isothermal at 165 °C during 3 min before cooling to 5 °C at the cooling rate of 2 °C/min. Because PEG in this sample rapidly crystallized, the sample was stored inside the DSC cell to ensure a well-controlled storage

condition for predetermined time periods and subsequently heating to 165 °C at 5 °C/min.

The DSC thermogram showing the reversing heat flow signal and the first derivative of the reversing heat flow signal of the dispersions containing 45% IMC upon storage is illustrated in Figure 9a and b, respectively. At the beginning, the dispersions showed a single  $T_g$  in the reversing heat flow signal reflected by a sharp peak in the derivative signal. Following storage up to 1 h, a single  $T_g$  was still shown, representing a homogeneous phase of amorphous PEG and IMC. The heat capacity ( $\Delta C_p$ ) jump at  $T_g$  or the area of the derivative reversing heat flow peak corresponding to this  $T_g$  (AUC) considerably decreased due to the crystallization of PEG.

Storage for 2 h onward led to the evolution of distinct regions corresponding to two  $T_g$ 's. This indicates amorphous–amorphous phase separation in the amorphous dispersions of PEG and IMC forming polymer-rich and drug-rich domains. The drug-rich domain was generated from the polymer-rich domain upon the crystallization of PEG, whereas amorphous IMC was still intact. The lower  $T_g$  ( $T_{g1}$ ) should be from the PEG-rich domain, whereas the higher  $T_g$  ( $T_{g2}$ ) represents the IMC-rich domain.

The drug–polymer separation in the dispersions appeared to continue upon further aging up to 8 h. It was apparent from the derivative reversing signal that  $T_{g1}$  was always observable at ca. -32 °C and displayed a decreasing  $\Delta C_{p1}$  whereas  $T_{g2}$  shifted to higher temperature and developed an increasing  $\Delta C_{p2}$  as a function of time (Figure 10). This can be explained by the fact that owing to the crystallization of the polymer while the drug remained amorphous, the PEG-rich domain decreased in size, whereas in the IMC-rich domain, both drug/polymer ratio as well as the domain size were increasing as revealed by a higher  $T_{g2}$  and  $\Delta C_{p2}$ .

$\Delta C_{p1}$  continued to decrease upon storage before  $T_{g1}$  became undetectable after 10 h of isothermal aging, demonstrating vanishing of the PEG-rich domain.  $T_{g2}$  increased as the drug/polymer ratio in the IMC-rich domain was still rising, whereas  $\Delta C_{p2}$  started to gradually decrease from 9 h because the decrease in amorphous polymer in this domain dominated the increase in amorphous drug and eventually the total size of drug-rich domain reduced.

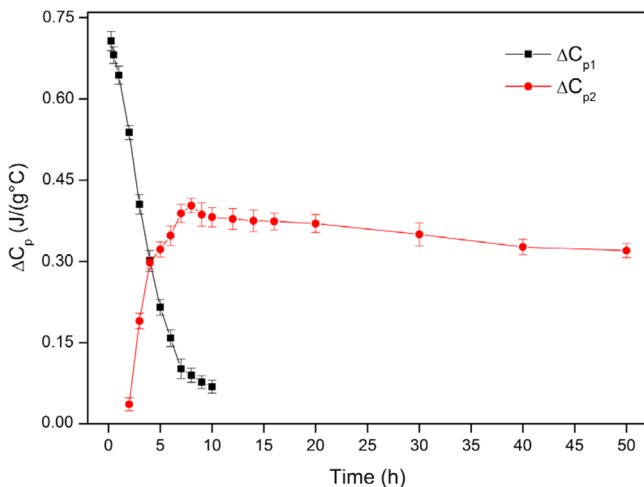


**Figure 10.** Change in heat capacity of the sample containing 45% IMC upon storage.

During the crystallization period,  $\Delta T_g$ 's width corresponding to  $T_{g1}$  and  $T_{g2}$  were virtually unaltered, signifying the homogeneous distribution of drug and polymer in both drug-rich and polymer-rich domains. Additionally, crystallization of IMC was excluded by the absence of diffraction peaks of IMC in the XRD diffractogram (Figure 11). After up to 50 h, only Bragg peaks of PEG were found, the intensity of which increased as a function of time.

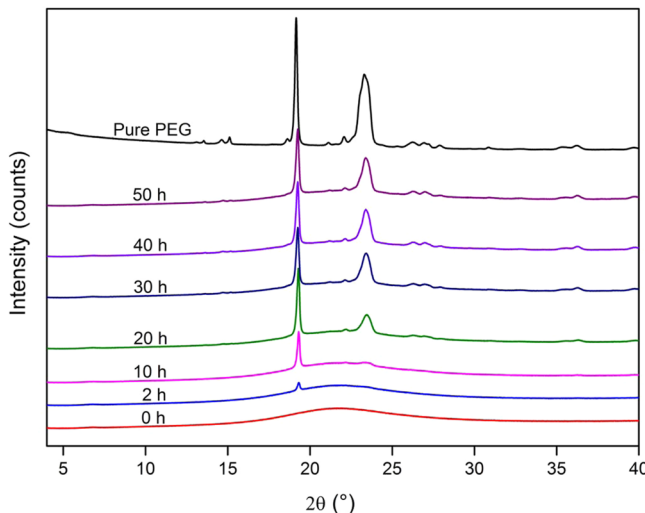


**Figure 11.** XRD diffractogram showing the evolution of diffraction peaks during the crystallization process of the sample containing 45% IMC upon storage.

A summary of the crystallization process of the sample containing 45% IMC upon storage is illustrated in Figure 12.

Similar trends in  $T_g$  shifts were likewise observed for samples containing higher IMC loadings. Due to the slower crystallization rate of PEG as the weight fraction of IMC was rising, it took more time for the amorphous–amorphous phase separation to take place. Although the IMC-rich domain became detectable after 2 h in the sample containing 45% IMC, it took 8 and 42 h for this domain to be generated in samples containing 50% and 55% IMC, respectively. It might well be possible that the amorphous–amorphous phase separation developed prior to these time points; however, it should be

noted that a phase separated domain must be large enough, that is greater than ca. 30 nm to be detected by the thermal changes measured by DSC.<sup>27</sup> Other techniques based on solid-state nuclear magnetic resonance spectroscopy are more sensitive than DSC to reveal phase separation.<sup>25,28,29</sup>

When the weight fraction of IMC increased to 60%, a single  $T_g$  was detected during the whole crystallization process, suggesting that amorphous–amorphous phase separation did not occur in this system. Because PEG crystallized very slowly in the presence of 60% drug loading, IMC molecules would probably have enough time to diffuse from drug-rich domain to polymer-rich domain as a result of concentration gradient, forming a single homogeneous dispersion of drug and polymer. The absence of amorphous–amorphous phase separation could also be expected for mixtures containing higher IMC loadings.

Table 3 shows the crystallinity of PEG in dispersions with IMC at the time points when the IMC-rich domain became detectable. The drug-rich domain was not visible in the DSC thermogram until at least 4.9% to 6.7% of amorphous PEG already crystallized.

**Temperature-Dependent Crystallinity of PEG.** For investigation of temperature-dependent crystallinity of PEG in dispersions, the mixture of PEG and IMC containing 45% drug loading was mounted on a TTK 450 thermostated sample holder unit (Anton Paar, Graz, Austria), kept isothermal at 165 °C during 3 min, followed by cooling to 5, 10, 20, and 25 °C at a cooling rate of 2 °C/min; then XRD diffractograms at these temperatures were recorded (Figure 13).

The intensity of the unique diffraction peak of PEG at 19.2° appeared to be inversely proportional to the final temperature. This peak decreased in intensity when the temperature increased, suggesting lower crystallinity of PEG when cooled to higher temperature. This observation was consistent with crystallization kinetics of PEG which was recently reported that PEG crystallized more slowly at 40 °C than at 25 °C, in both pure material and in solid dispersions with various APIs.<sup>11</sup> This can be explained by the decrease in the extent of supercooling of PEG at higher crystallization temperature, which in turn decreases the driving force for nucleation and, hence, the crystallization rate.

## DISCUSSION

It is well known for solid dispersions that phase separation often occurs as the drug weight fraction increases. This work clearly shows the opposite: increasing IMC weight fraction results in higher stability of drug-carrier system. The amorphization effect of IMC on PEG in this study is in good agreement with previous reports that IMC tends to increase the degree of amorphicity of solid dispersions with PEG.<sup>30–33</sup> APIs such as temazepam<sup>22</sup> have been found to inhibit the solidification of PEG, whereas other molecules enhanced (e.g., phenylbutazone<sup>31</sup>) or had no influence (e.g., triamterene<sup>22</sup>) on the crystallinity of the polymer. In recent studies, Zhu et al. showed that ibuprofen, benzocaine, chlorpropamide, and aceclofenac decreased the growth rate of PEG because these compounds formed hydrogen bonds with the polymer, whereas haloperidol and fenofibrate had almost no effect on crystallization rate of PEG as they lacked donor groups to interact with acceptor groups of the polymer.<sup>3,11</sup> Despite the fact that ibuprofen and benzocaine could impede the crystal growth of PEG through hydrogen bonding, the polymer still crystallized very rapidly within few minutes. The role of intermolecular interactions between an amorphous component

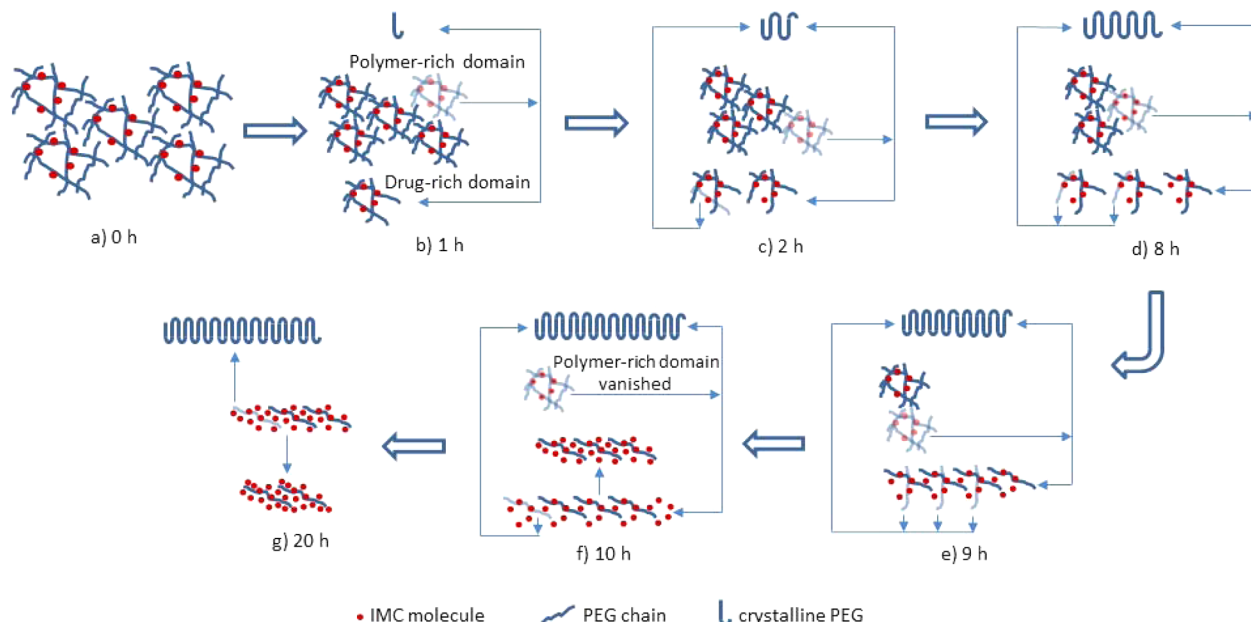


**Figure 12.** Overview of the crystallization process of the sample containing 45% IMC upon storage. (a) Freshly prepared dispersion shows a single  $T_g$ . (b) After 1 h of storage, a single  $T_g$  is still observed but its  $\Delta C_p$  drops due to the crystallization of amorphous PEG. (c) After 2 h, the crystallization of PEG generates polymer-rich domain and detectable drug-rich domain as shown by two distinct  $T_g$ 's. (d) After 8 h, the amorphous–amorphous phase separation progresses.  $T_{g1}$  remains unchanged whereas  $T_{g2}$  shifts to higher temperature.  $\Delta C_{p1}$  decreases, whereas  $\Delta C_{p2}$  increases. (e) After 9 h,  $T_{g1}$  remains unaltered, whereas  $\Delta C_{p1}$  continues to decrease.  $T_{g2}$  increases as the drug/polymer ratio in the IMC-rich domain is still rising, whereas  $\Delta C_{p2}$  decreases because the decrease in amorphous polymer in this domain dominates the increase in amorphous drug and eventually the total size of drug-rich domain reduces. (f) After 10 h, the polymer-rich domain becomes undetectable.  $T_{g2}$  keeps increasing, whereas  $\Delta C_{p2}$  continues to decrease. (g) After 20 h, the same trend as after 10 h is observed, but the crystallization process becomes slower.

**Table 3. Crystallinity of PEG in Dispersions Containing Various Drug Loadings at the Time Points When the IMC-Rich Domain Is Detectable**

time (hour)	crystallinity of PEG (%)			
	45%	50%	55%	60%
1	3.7	—	—	—
2	11.6 <sup>a</sup>	—	—	—
6	—	4.9	—	—
8	—	6.7 <sup>a</sup>	—	—
24	—	—	3.3	—
42	—	—	7.8 <sup>a</sup>	—
264	—	—	—	—
288	—	—	—	—

<sup>a</sup>Drug-rich domain is detectable.

and a crystalline polymer in decreasing the growth rate of the polymer was also reported for semicrystalline polymer blends.<sup>7,34</sup>

In miscible polymer blends of an amorphous polymer and a (semi)crystalline polymer, the amorphous additive can be excluded from the crystalline polymer, generating various types of morphology depending on the distance of the amorphous phase segregation. These types of morphology include (1) interlamellar, where segregation of amorphous component develops at lamellar level and the additive is located in the interlamellar regions, (2) interfibrillar, where the additive is segregated by a larger distance and resides between lamellar stacks, and (3) interspherulitic, where the additive is segregated by the largest distance to the zones between spherulites (Figure 14). The additive does not necessarily have to be located in a single zone but may reside in multiple regions in one blend.<sup>35</sup>

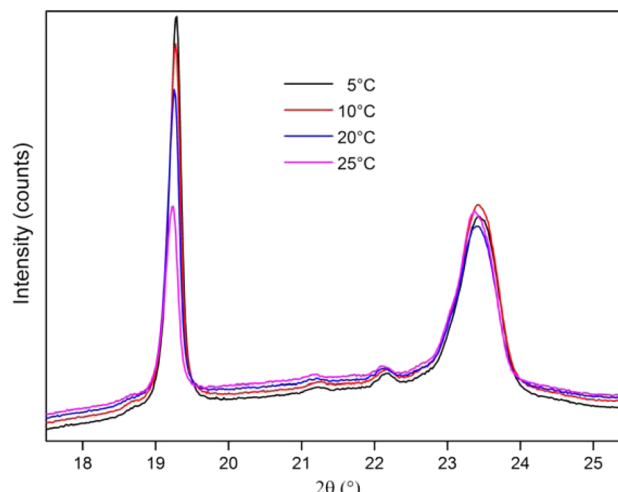


**Figure 13.** XRD diffractogram of the sample containing 45% IMC at different final temperatures.

Segregation of an amorphous additive from a crystalline polymer might take place as the result of thermodynamic and kinetic driving forces. The confinement of an additive in interlamellar regions of a crystalline polymer is entropically unfavorable since polymer crystals can deform the additive molecules and hence decrease conformational entropy. An entropic driving force that favors random coil conformation, therefore, is developed to liberate the additive molecules from interlamellar regions.<sup>10</sup> Beside the entropic driving force, a crystallization driving force of crystallizable segments within interlamellar regions which depends on the degree of supercooling can play a role in exclusion of the additive from

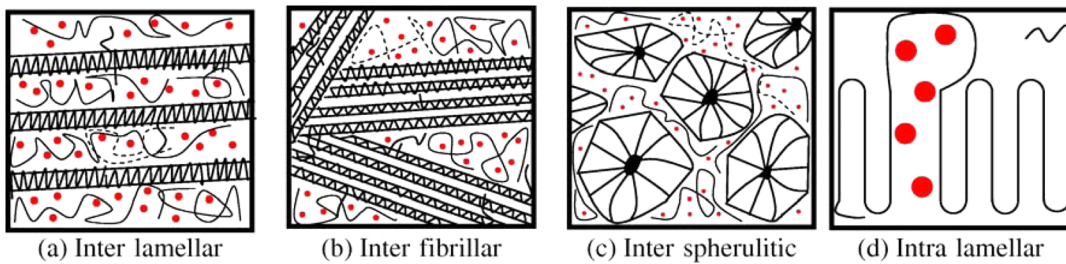


**Figure 14.** Possible mechanisms of segregation in drug/PEG mixture. Reprinted with permission from the work of Yang et al.<sup>40</sup>

these regions. In addition to these two thermodynamic forces, intermolecular interactions between the two components as well as diffusivity of the additive molecules could also influence the segregation of an amorphous additive from a crystalline polymer. Stronger intermolecular interactions between two components in miscible blends decrease the crystal growth rate of crystalline polymer, which slows down the segregation process and results in more time for the amorphous component to diffuse away from the interlamellar regions. If the diffusion rate of the amorphous additive is relatively slower than the crystal growth rate of the crystalline polymer, additive molecules may be confined inside interlamellar regions before they have a chance to diffuse out.<sup>36</sup> The segregation of an amorphous additive from a crystalline polymer, thus, is governed by the interplay between entropic and crystallization driving forces, intermolecular interactions between amorphous additive, and crystalline polymer as well as diffusivity of the additive molecule.

The crystallization process of PEG requires the folding of random coil polymer chains into small clusters before these clusters gather and coalesce into lamellae.<sup>37–39</sup> Yang et al. recently showed that incorporation of acetaminophen, a low molecular weight API into drug–PEG systems makes the PEG chains behave in a less flexible fashion, and hence, the initial step of chain folding in the crystallization process becomes more difficult to occur.<sup>40</sup> Accordingly, IMC molecules, which may potentially reside in interlamellar/intralamellar regions of polymer hinder the diffusion and packaging of PEG chains. In addition, increasing the drug loading leads to a clearly observable higher viscosity of the system, as originated from the decrease in molecular mobility, which restricts any diffusional transport process required for nucleation and crystal growth.

In a recent study, Zhu et al. reported that in solid dispersions with fenofibrate (FNB), a drug which exhibits several characteristics similarly to IMC such as slow crystallization tendency and limited ability to interact with PEG, the crystallization rate of PEG is almost the same as for pure PEG.<sup>11</sup> Both IMC and FNB belong to the Class III in the classification scheme of crystallization tendency of organic molecules proposed by Baird et al., that is, having good glass forming ability and high glass stability.<sup>41</sup> From the time–temperature–transformation diagram, Karmwar et al. showed that amorphous IMC could be prepared from the melt at a minimum cooling rate of 1.2 °C/min.<sup>23</sup> Fukuoka et al.<sup>42</sup> and Ayenew et al.<sup>43</sup> were able to generate amorphous IMC at even lower cooling rate down to 0.67 °C/min and 0.2 °C/min, respectively. In addition, IMC and fenofibrate are both small molecules with relatively complex structure containing numerous rotatable bonds and hence exhibiting low probability of being in the proper orientation to undergo nucleation.<sup>41,44,45</sup>

The two API are also more or less comparable in terms of various physicochemical properties, which might dictate the crystallization tendency such as reduced glass transition temperature ( $T_g/T_m$ ), heat of fusion, entropy of fusion, density, enthalpy of structural relaxation and configurational heat capacity.<sup>41</sup> However, the solubilization effect of IMC on PEG was not observed with FNB as well as other APIs in the Class III including itraconazole, ketoconazole, and miconazole. Therefore, additional factors that have not yet been elucidated rather than aforementioned physicochemical properties should play a role to cause the difference in influence of API on crystallization kinetics of the polymer in dispersions with PEG. In API/PEG solid dispersions, it was previously hypothesized that drugs could be molecularly dispersed into the crystalline moieties of PEG and solid solutions of drugs in PEGs were considered to be interstitial.<sup>46</sup> Later, however, it was observed that molecularly dispersed drugs reside predominantly in the amorphous domains of PEG.<sup>47–49</sup> The miscibility between API and PEG is dependent on these amorphous domains of the polymer. Therefore, the influence of API on crystallization of amorphous PEG is crucial for the phase stability of API/PEG solid dispersions.

It has been found in the current work that for IMC/PEG dispersions, crystallization of PEG results in destabilization of amorphous IMC. In addition, when IMC starts crystallizing, it facilitates the polymer to crystallize as well. IMC and PEG stabilize each other in the amorphous system even without forming hydrogen bonding as reported by Ford et al.,<sup>31</sup> Fini et al.<sup>32</sup> and Valizadeh et al.<sup>33</sup> The crystallization of drug or polymer is the driving force for the crystallization of the other component.

From the crystallization kinetics of PEG (Figure 8), it was obvious that higher drug loading slowed down crystallization of the polymer. However, when IMC started crystallizing, it crystallized faster in samples containing higher drug loadings even though the amorphous fraction of PEG in these samples was larger. At 60% IMC, Bragg peaks of crystalline IMC were detected before the end point of PEG crystallization whereas for samples containing lower drug weight fraction, no evidence of IMC crystals was found until crystallization of PEG had finished. This can be explained by the fact that when PEG crystals were generated, they could act as heterogeneous nucleation surfaces for crystallization of IMC, as similarly observed for crystallization of ibuprofen and fenofibrate at the interface between molten drug and crystalline PEG.<sup>11</sup> For samples containing more drug content (60%), higher local concentration of drug is presented which results in faster nucleation of API on the surface of PEG crystals. Amorphous IMC is reported to be stable against crystallization even for two years.<sup>50</sup> In dispersions with PEG, due to the heterogeneous nucleation of IMC promoted by PEG nucleation surfaces, IMC

crystallizes faster than in the pure state, which is unexpected for solid dispersions. Accordingly, crystallization kinetics of drug–PEG dispersions is the result of the interplay between numerous factors including crystallization tendency of the drug and its ability to interact with PEG, mobility of the API molecule,<sup>7</sup> crystallization temperature as well as additional complicating factors such as heterogeneous nucleation promoted by PEG.

After almost 3 weeks of storage at 5 °C, not more than a half of the amorphous fraction of PEG crystallized (Table 2). It can be proposed that the rest of amorphous PEG will continue to crystallize during storage, but at significantly lower rate, until the crystallinity of PEG in dispersions with IMC reaches the value of the raw material (ca. 86%). In other words, PEG exhibits biphasic crystallization behavior in dispersions with IMC: an initial fast phase within few weeks and a second slow phase within months or even years.

It is still unknown whether the solubilization effect of IMC on PEG depends on molecular weight and chain length of PEG because the differences in these parameters may result in various spherulite growth rate,<sup>51</sup> crystallization,<sup>52</sup> and solidification rate<sup>22</sup> as well as lamellar structure,<sup>53</sup> crystallinity,<sup>54</sup> viscosity of the polymer,<sup>55</sup> and drug–polymer miscibility.<sup>56</sup>

Amorphous–amorphous phase separation which exhibits two  $T_g$ 's representing polymer-rich and drug-rich domains was observed for IMC/PEG dispersions containing up to 55% drug loading, whereas no phase separation occurred in the sample containing at least 60% IMC. This is most likely due to the interplay between the two factors namely crystallization rate of PEG and diffusion rate of IMC. In drug–polymer mixtures containing 60% IMC, PEG crystallizes very slowly and the crystallization rate of PEG is probably relatively lower than the diffusion rate of IMC. The gradual crystallization of amorphous PEG, whereas amorphous IMC is still intact produces regions with different drug concentrations. Therefore, the concentration gradient generates a flux of IMC molecules from a region of higher drug concentration to one of lower drug concentration, redistributing IMC in amorphous PEG and forming a single homogeneous amorphous phase. At lower drug loadings of not more than 55% where amorphous PEG crystallizes faster, the diffusion rate of the drug might be lower than the crystallization rate of the polymer. Consequently, there is insufficient time for the IMC molecules to redistribute in amorphous polymer, resulting in the evolution of polymer-rich and drug-rich domains.

## CONCLUSIONS

Crystallization kinetics of IMC/PEG solid dispersions containing high drug loadings were characterized by DSC and XRD. For the first time, it has been elaborately shown that a small drug molecule can completely transform a semicrystalline polymer into the amorphous state. Increasing the weight fraction of drug results in higher stability and slows down the crystallization rate of the amorphous polymer. Drug loading seems to influence the microstructure of dispersions by changing the polymer crystallization rate. Depending on the variation between the crystallization rate of PEG and the diffusion rate of IMC, the crystallization of the polymer may produce a single amorphous phase or generate amorphous–amorphous phase separation, forming polymer-rich domain and drug-rich domain which exhibits distinct glass transition temperatures. The current study helps to explain the large variation in the physicochemical properties of API/PEG

dispersions as a function of drug loading. Given the complex nature of API/PEG dispersions, which are governed by the interplay between numerous factors, these observations are important for preparation of solid dispersions with reproducible and consistent physicochemical properties and pharmaceutical performance.

## AUTHOR INFORMATION

### Corresponding Author

\*E-mail: Guy.VandenMooter@pharm.kuleuven.be. Tel.: +32 16 330 304. Fax: +32 16 330 305.

### Author Contributions

The manuscript was written through contributions of all authors. All authors have given approval to the final version of the manuscript.

### Notes

The authors declare no competing financial interest.

## ACKNOWLEDGMENTS

The authors acknowledge the financial support from FWO-Vlaanderen (G.0764.13). Tu Van Duong gratefully acknowledges the scholarship awarded by FWO-Vlaanderen (G.0764.13).

## ABBREVIATIONS

API, active pharmaceutical ingredient; PEG, polyethylene glycol; IMC, indomethacin; MDSC, modulated differential scanning calorimeter; XRD, X-ray diffraction;  $C_p$ , heat capacity; AUC, area under the derivative reversing heat flow peak;  $T_g$ , glass transition temperature;  $T_m$ , melting point; FNB, fenofibrate

## REFERENCES

- (1) Leuner, C.; Dressman, J. Improving drug solubility for oral delivery using solid dispersions. *Eur. J. Pharm. Biopharm.* **2000**, *50* (1), 47–60.
- (2) Lin, C. W.; Cham, T. M. Effect of particle size on the available surface area of nifedipine from nifedipine-polyethylene glycol 6000 solid dispersions. *Int. J. Pharm.* **1996**, *127* (2), 261–272.
- (3) Zhu, Q.; Taylor, L. S.; Harris, M. T. Evaluation of the microstructure of semicrystalline solid dispersions. *Mol. Pharmaceutics* **2010**, *7* (4), 1291–1300.
- (4) Gines, J.; Arias, M.; Moyano, J.; Sanchez-Soto, P. Thermal investigation of crystallization of polyethylene glycols in solid dispersions containing oxazepam. *Int. J. Pharm.* **1996**, *143* (2), 247–253.
- (5) Zhu, Q.; Toth, S. J.; Simpson, G. J.; Hsu, H.-Y.; Taylor, L. S.; Harris, M. T. Crystallization and dissolution behavior of naproxen/polyethylene glycol solid dispersions. *J. Phys. Chem. B* **2013**, *117* (5), 1494–1500.
- (6) Unga, J.; Matsson, P.; Mahlin, D. Understanding polymer–lipid solid dispersions—The properties of incorporated lipids govern the crystallisation behaviour of PEG. *Int. J. Pharm.* **2010**, *386* (1), 61–70.
- (7) Talibuddin, S.; Wu, L.; Runt, J. Microstructure of melt-miscible, semicrystalline polymer blends. *Macromolecules* **1996**, *29*, 7527.
- (8) Silvestre, C.; Cimmino, S.; Martuscelli, E.; Karasz, F.; MacKnight, W. Poly(ethylene oxide)/poly(methyl methacrylate) blends: influence of tacticity of poly(methyl methacrylate) on blend structure and miscibility. *Polymer* **1987**, *28* (7), 1190–1199.
- (9) Cimmino, S.; Di Pace, E.; Martuscelli, E.; Silvestre, C. Poly(ethylene oxide)/poly(methyl methacrylate) blends: Influence of tacticity of PMMA on the radial growth rate of PEO spherulites. *Macromol. Rapid Commun.* **1988**, *9* (4), 261–265.

- (10) Russell, T.; Ito, H.; Wignall, G. Neutron and X-ray scattering studies on semicrystalline polymer blends. *Macromolecules* **1988**, *21* (6), 1703–1709.
- (11) Zhu, Q.; Harris, M. T.; Taylor, L. S. Modification of crystallization behavior in drug/polyethylene glycol solid dispersions. *Mol. Pharmaceutics* **2012**, *9* (3), 546–553.
- (12) Owusu-Ababio, G.; Ebube, N. K.; Reams, R.; Habib, M. Comparative dissolution studies for mefenamic acid-polyethylene glycol solid dispersion systems and tablets. *Pharm. Dev. Technol.* **1998**, *3* (3), 405–412.
- (13) Ford, J.; Rubinstein, M. Formulation and ageing of tablets prepared from indomethacin-polyethylene glycol 6000 solid dispersions. *Pharm. Acta Helv.* **1980**, *55* (1), 1–7.
- (14) Margarit, M. V.; Rodríguez, I. C.; Cerezo, A. Physical characteristics and dissolution kinetics of solid dispersions of ketoprofen and polyethylene glycol 6000. *Int. J. Pharm.* **1994**, *108* (2), 101–107.
- (15) Vidotto, G.; Levy, D.; Kovacs, A. Cristallisation et fusion des polymères autoensemencés. *Colloid Polym. Sci.* **1969**, *230* (2), 289–305.
- (16) Avrami, M. Kinetics of phase change. I General theory. *J. Chem. Phys.* **1939**, *7* (12), 1103–1112.
- (17) Avrami, M. Kinetics of phase change. II Transformation-time relations for random distribution of nuclei. *J. Chem. Phys.* **1940**, *8*, 212–224.
- (18) Avrami, M. Granulation, phase change, and microstructure kinetics of phase change. III. *J. Chem. Phys.* **1941**, *9*, 177–184.
- (19) Vasa, D. M.; Dalal, N.; Katz, J. M.; Roopwani, R.; Nevrekar, A.; Patel, H.; Buckner, I. S.; Wildfang, P. L. Physical characterization of drug: polymer dispersion behavior in polyethylene glycol 4000 solid dispersions using a suite of complementary analytical techniques. *J. Pharm. Sci.* **2014**, *103* (9), 2911–2923.
- (20) Faucher, J.; Koleske, J.; Santee, E., Jr; Stratta, J.; Wilson, C., III Glass transitions of ethylene oxide polymers. *J. Appl. Phys.* **1966**, *37* (11), 3962–3964.
- (21) Jackson, K.; Uhlmann, D. R.; Hunt, J. On the nature of crystal growth from the melt. *J. Cryst. Growth* **1967**, *1* (1), 1–36.
- (22) Dordunoo, S. K.; Ford, J. L.; Rubinstein, M. H. Solidification studies of polyethylene glycols, gelucire 44/14 or their dispersions with triamterene or temazepam. *J. Pharm. Pharmacol.* **1996**, *48* (8), 782–789.
- (23) Karmwar, P.; Bøtker, J. P.; Graeser, K.; Strachan, C.; Rantanen, J.; Rades, T. Investigations on the effect of different cooling rates on the stability of amorphous indomethacin. *Eur. J. Pharm. Sci.* **2011**, *44* (3), 341–350.
- (24) Song, M.; Hammiche, A.; Pollock, H.; Hourston, D.; Reading, M. Modulated differential scanning calorimetry: 4. Miscibility and glass transition behaviour in poly(methyl methacrylate) and poly(epichlorohydrin) blends. *Polymer* **1996**, *37* (25), 5661–5665.
- (25) Mandelkern, L. *Crystallization of Polymers: Vol. 2, Kinetics and Mechanisms*, 2nd ed.; Cambridge University Press: New York, 2004; p 19.
- (26) Mihailov, M.; Nedkov, E.; Goshev, I. Temperature dependence of morphology of supermolecular structures growing in the thin layer melt of fractions of poly(ethylene oxide). *J. Macromol. Sci., Part B: Phys.* **1978**, *15* (2), 313–328.
- (27) Krause, S.; Iskandar, M. *Phase separation in styrene- $\alpha$ -methyl styrene block copolymers*; Springer: New York, 1977; pp 231–243.
- (28) Ivanisevic, I.; Bates, S.; Chen, P. Novel methods for the assessment of miscibility of amorphous drug-polymer dispersions. *J. Pharm. Sci.* **2009**, *98* (9), 3373–3386.
- (29) Pham, T. N.; Watson, S. A.; Edwards, A. J.; Chavda, M.; Clawson, J. S.; Strohmeier, M.; Vogt, F. G. Analysis of amorphous solid dispersions using 2D solid-state NMR and  $^1\text{H}$  T1 relaxation measurements. *Mol. Pharmaceutics* **2010**, *7* (5), 1667–1691.
- (30) Ford, J.; Rubinstein, M. Ageing of indomethacin-polyethylene glycol 6000 solid dispersion. *Pharm. Acta Helv.* **1978**, *54* (12), 353–358.
- (31) Ford, J. L.; Stewart, A. F.; Dubois, J.-L. The properties of solid dispersions of indomethacin or phenylbutazone in polyethylene glycol. *Int. J. Pharm.* **1986**, *28* (1), 11–22.
- (32) Fini, A.; Rodriguez, L.; Cavallari, C.; Albertini, B.; Passerini, N. Ultrasound-compacted and spray-congealed indomethacin/polyethylene glycol systems. *Int. J. Pharm.* **2002**, *247* (1), 11–22.
- (33) Valizadeh, H.; Nokhodchi, A.; Qaraqhani, N.; Zakeri-Milani, P.; Azarmi, S.; Hassanzadeh, D.; Löbenberg, R. Physicochemical characterization of solid dispersions of indomethacin with PEG 6000, Myrl 52, lactose, sorbitol, dextrin, and Eudragit® E100. *Drug Dev. Ind. Pharm.* **2004**, *30* (3), 303–317.
- (34) Kuo, S. W.; Chan, S. C.; Chang, F. C. Effect of hydrogen bonding strength on the microstructure and crystallization behavior of crystalline polymer blends. *Macromolecules* **2003**, *36* (17), 6653–6661.
- (35) Stein, R.; Khambatta, F.; Warner, F.; Russell, T.; Escala, A.; Balizer, E. X-ray and optical studies of the morphology of polymer blends. *J. Polym. Sci., Polym. Symp.* **1978**, *63*, 313–328.
- (36) Chen, H. L.; Li, L. J.; Lin, T. L. Formation of segregation morphology in crystalline/amorphous polymer blends: molecular weight effect. *Macromolecules* **1998**, *31* (7), 2255–2264.
- (37) Kovacs, A.; Gonthier, A.; Straupe, C. Isothermal growth, thickening, and melting of poly(ethylene oxide) single crystals in the bulk. *J. Polym. Sci., Polym. Symp.* **1975**, *50*, 283–325.
- (38) Hoffman, J. D.; Miller, R. L. Kinetic of crystallization from the melt and chain folding in polyethylene fractions revisited: theory and experiment. *Polymer* **1997**, *38* (13), 3151–3212.
- (39) Yamamoto, T. Molecular dynamics simulation of polymer crystallization through chain folding. *J. Chem. Phys.* **1997**, *107* (7), 2653–2663.
- (40) Yang, M.; Gogos, C. Crystallization of poly(ethylene oxide) with acetaminophen—A study on solubility, spherulitic growth, and morphology. *Eur. J. Pharm. Biopharm.* **2013**, *85* (3), 889–897.
- (41) Baird, J. A.; Van Eerdenbrugh, B.; Taylor, L. S. A classification system to assess the crystallization tendency of organic molecules from undercooled melts. *J. Pharm. Sci.* **2010**, *99* (9), 3787–3806.
- (42) Fukuoka, E.; Makita, M.; Yamamura, S. Some physicochemical properties of glassy indomethacin. *Chem. Pharm. Bull.* **1986**, *34* (10), 4314–4321.
- (43) Ayenew, Z.; Paudel, A.; Rombaut, P.; Van den Mooter, G. Effect of compression on non-isothermal crystallization behaviour of amorphous indomethacin. *Pharm. Res.* **2012**, *29* (9), 2489–2498.
- (44) Yu, L.; Reutzel-Edens, S. M.; Mitchell, C. A. Crystallization and polymorphism of conformationally flexible molecules: Problems, patterns, and strategies. *Org. Process Res. Dev.* **2000**, *4* (5), 396–402.
- (45) Trasi, N. S.; Baird, J. A.; Kestur, U. S.; Taylor, L. S. Factors influencing crystal growth rates from undercooled liquids of pharmaceutical compounds. *J. Phys. Chem. B* **2014**, *118* (33), 9974–9982.
- (46) Chiou, W. L.; Riegelman, S. Pharmaceutical applications of solid dispersion systems. *J. Pharm. Sci.* **1971**, *60* (9), 1281–1302.
- (47) Schachter, D. M.; Xiong, J.; Tirol, G. C. Solid state NMR perspective of drug–polymer solid solutions: a model system based on poly(ethylene oxide). *Int. J. Pharm.* **2004**, *281* (1), 89–101.
- (48) Yeh, F.; Hsiao, B. S.; Chu, B.; Sauer, B. B.; Flexman, E. A. Effect of miscible polymer diluents on the development of lamellar morphology in poly(oxyethylene) blends. *J. Polym. Sci., Part B: Polym. Phys.* **1999**, *37* (21), 3115–3122.
- (49) Dreezen, G.; Ivanov, D.; Nysten, B.; Groeninckx, G. Nanostructured polymer blends: phase structure, crystallisation behaviour and semi-crystalline morphology of phase separated binary blends of poly(ethylene oxide) and poly(ether Sulphone). *Polymer* **2000**, *41* (4), 1395–1407.
- (50) Wojnarowska, Z.; Adrjanowicz, K.; Włodarczyk, P.; Kaminska, E.; Kaminski, K.; Grzybowska, K.; Wrzalik, R.; Paluch, M.; Ngai, K. Broadband dielectric relaxation study at ambient and elevated pressure of molecular dynamics of pharmaceutical: indomethacin. *J. Phys. Chem. B* **2009**, *113* (37), 12536–12545.

- (S1) Maclaine, J.; Booth, C. Effect of molecular weight on spherulite growth rates of high molecular weight poly(ethylene oxide) fractions. *Polymer* **1975**, *16* (3), 191–195.
- (S2) Godovsky, Y. K.; Slonimsky, G.; Garbar, N. Effect of molecular weight on the crystallization and morphology of poly(ethylene oxide) fractions. *J. Polym. Sci. C, Polym. Symp.* **1972**, *38*, 1–21.
- (S3) Spegt, P. P. Rôle de la masse moléculaire sur la structure lamellaire des polyoxyéthylenes. *Macromol. Chem. Phys.* **1970**, *140* (1), 167–177.
- (S4) Connor, T.; Read, B.; Williams, G. The dielectric, dynamic mechanical and nuclear resonance properties of polyethylene oxide as a function of molecular weight. *J. Appl. Chem.* **1964**, *14* (2), 74–81.
- (S5) Teramoto, A.; Fujita, H. Temperature and molecular weight dependence of the melt viscosity of polyethylene oxide in bulk. *Macromol. Chem. Phys.* **1965**, *85* (1), 261–272.
- (S6) Janssens, S.; Denivelle, S.; Rombaut, P.; Van den Mooter, G. Influence of polyethylene glycol chain length on compatibility and release characteristics of ternary solid dispersions of itraconazole in polyethylene glycol/hydroxypropylmethylcellulose 2910 E5 blends. *Eur. J. Pharm. Sci.* **2008**, *35* (3), 203–210.